

External Control of Electron Temperature in Ultra-Cold Plasmas

Roy O. Wilson and Duncan A. Tate

Department of Physics and Astronomy, Colby College, Waterville, ME 04901

Abstract. We discuss our progress towards achieving external control of the electron temperature and the Coulomb coupling parameter of ultra-cold plasmas. Using a Littman dye laser, we create the plasma by partially photoionizing a dense, cold sample of rubidium atoms in a magneto-optical trap (MOT). At a controllable time delay, we excite neutral atoms in the plasma to a specific Rydberg state using a narrow bandwidth pulsed laser. We have made very qualitative measurements of the electron temperature as a function of delay from the exciting laser pulses. Some of our results suggest that the plasma is stabilized by the presence of the Rydberg atoms, with a longer lifetime and slower expansion rate than a plasma that evolves directly from a dense Rydberg sample.

Keywords: Atomic and Molecular Physics

PACS: 33.80.Ps, 33.80.Rv, 52.25.Ya, 52.27.Gr

INTRODUCTION

The creation of an almost electrically neutral ultracold, strongly coupled plasma was first reported several years ago [1]. Such a plasma is an exciting environment from the theoretical point of view, since the electrostatic interaction energy of the electrons and ions become comparable to their kinetic energies. These plasmas are created by photoionization of atoms in a magneto-optical trap (MOT) using a pulsed laser (pulse duration ≈ 10 ns). So far, plasmas have been created using using cold Xe, Rb, Cs, and Sr atoms [1, 2, 3, 4], as well as in cold samples of other atoms. The initial electron temperature (0.1 - 1000 K) is determined by the excess photon energy above the ionization limit of the photoionizing laser, due to the large mass difference between the electron and the ion and the need to conserve momentum during the ionization process. On the other hand, the initial positive ion energy is that of the initially trapped atoms before ionization (100 μ K). After a first burst of photoelectrons leaves the laser-atom interaction region, the excess positive charge of the ions traps the remaining electrons and the plasma forms. The plasma has been estimated to be almost neutral, with at most a 5% excess of positive charge. Collisions between electrons, ions, and neutral atoms thermalize the plasma, and three-body (dielectronic) recombination results in formation of Rydberg states and heating of the electrons, which evaporate from the plasma as it expands slowly on a time scale of ~ 100 μ s due to Coulomb forces. In addition, electron-Rydberg atom scattering can both heat and cool the electrons. This environment has been the subject of several theoretical papers that were stimulated by the initial experimental observation [5, 6, 7, 8, 9, 10].

Soon after the initial creation of an ultracold plasma from cold atoms in a MOT, a related phenomenon was observed, in which cold Rydberg Rb or Cs atoms in a MOT

were then found to evolve spontaneously to plasma on a time scale of $\sim 1 \mu\text{s}$. The evolution happens when the atom density is sufficiently high in states with $n^* > 25$, despite the fact that each atom may be bound by as much as 100 cm^{-1} [11, 12]. This discovery was made concurrently at University of Virginia (UVA), and at Laboratoire Aimé Cotton, Orsay, France (LAC), and reported a paper by Robinson *et al.* [11]. Further observations on the evolution of cold Rydberg atoms to plasma and a discussion of its relation with creation of Rydberg atoms in an ultracold plasma were reported by Gallagher *et al.* [12]. In these experiments, a Rydberg ns or nd state is populated in 10 ns by a pulsed laser from atoms in a MOT. After a small amount of initial ionization of Rydberg atoms occurs, electrons so formed leave the interaction region, and the net positive charge traps subsequently freed electrons. An ultracold, almost neutral plasma forms, that has a lifetime limited by the expansion of the ultracold ions to about 1 ms. During the slow expansion of the plasma, rapid (and apparently complete) ionization of Rydberg atoms occurs after $\sim 1 \mu\text{s}$. (This regime has been termed the “avalanche”, in contrast with the “pre-avalanche” initial stage of the evolution when ionization rates are low.) The resulting cold plasma expands slowly and the most energetic electrons evaporate as the ion potential well gets shallower.

Subsequent experiments carried out at UVA, and also parallel work at LAC, revealed the mechanisms by which the energy necessary to ionize the Rydberg atoms is supplied, and the cause of the initial ionization [13]. The initial ionization was found to be dominated by Rydberg-Rydberg collisions, rather than black body photoionization. Somewhat surprisingly, the collision process dominates even in the complete absence of hot Rydberg atoms, which had been thought to be critical to the initiation of the evolution to plasma [11]. (Further work at UVA revealed the role of dipole forces in changing the cold atom dynamics to cause ionizing collisions [14, 15].) The plasma evolution dynamics in the avalanche regime was found to be determined by electron-Rydberg scattering, leading to redistribution of Rydberg population to n and ℓ states different from that originally populated by the laser. As predicted theoretically [6], it was found that approximately 2/3 of the initial Rydberg sample ultimately ionized, while the other 1/3 was redistributed to lower energy states, thereby maintaining the energy balance in the system [13].

The effective “figures of merit” for plasmas (whether formed by direct photoionization, or by evolution from a plasma) are the so-called Coulomb coupling parameters (CCP’s) of the electrons, Γ_e , and of the positive ions, Γ_i [16]. These parameters measure the mean electrostatic interaction energy as a fraction of the kinetic energy, for each species. For the electrons,

$$\Gamma_e = \frac{e^2}{4\pi\epsilon_0 a k_B T_e}, \quad (1)$$

(where a the mean separation of the electrons, and T_e is the electron temperature), has been shown theoretically to reach an asymptotic value of order 0.2 in ultracold plasmas with no cooling mechanism [5]. (For $\Gamma_e > 1$, long range order effects, such as crystallization, may occur.) Clearly, the ability to cool the plasma by removing energy from the electrons is one factor that may push a plasma into the regime where $\Gamma_e > 1$.

In a recent theory paper, it was predicted that a certain amount of control over the plasma temperature (and therefore Γ_e) is possible using Rydberg atoms embedded into the plasma. If electron scattering from Rydberg atoms can be made to favor events where the Rydberg atom is excited to a higher energy state, thereby removing kinetic energy from the electrons, there is the possibility of pushing the electrons into the strongly coupled regime, $\Gamma_e \approx 1$ [17]. In particular, if another degree of experimental freedom is allowed, namely adding Rydbergs at times of order $1 \mu\text{s}$ after the plasma is excited, a quite dramatic enhancement of Γ_e is possible.

EXPERIMENTAL

The remainder of this paper describes our own preliminary experiments on the feasibility of temperature control of an ultra cold plasma using Rydberg atoms. In this section, we describe our apparatus. Two things should be pointed out. First, a precise measurement of the electron temperature is presently beyond our capabilities. We intend to ultimately use the “electron spilling” technique pioneered by Rolston’s group at NIST [18], and have done some preliminary experiments to that end. However, the temperature measurements described here are highly qualitative. Second, the maximum delay between exciting the plasma and the Rydberg atoms that we can achieve is 15 ns, limited by an optical delay line. For delays much longer than this, it is necessary to use two pump lasers triggered at the appropriate relative times, one which pumps the laser that creates the plasma, and one that pumps the laser that creates the Rydberg atoms. This also is beyond our present capability.

Magneto-Optical Trap

Our apparatus is basically a vapor-cell MOT [19] with internal field plates to allow electric fields to be applied to the atoms, plus a micro channel plate detector (MCP) [20, 21]. A vapor of rubidium atoms is contained in a stainless steel vacuum chamber in the form of a cylinder of diameter 150 mm and height 200 mm. The chamber is pumped by a 20 liter/s ion pump and has a base pressure of less than 1×10^{-9} torr. There is ample optical access for the trapping laser beams, as well as for pulsed lasers. There is a magnetic field gradient of up to 20 Gauss/cm in the center of the chamber, created by a pair of anti-Helmholtz coils on the outside of the chamber which are air-cooled when in use.

The Rb atoms are cooled by three orthogonal, retro-reflected laser beams of the appropriate circular polarizations. These beams are derived from a single external cavity diode laser [22] that is locked to the appropriate hyperfine component of the $5s_{1/2} \rightarrow 5p_{3/2}$ transition. This light is amplified (after suitable isolation measures) by an injection-locked non-cavity diode laser, expanded to a diameter of 10 mm, and split into the three orthogonal beams that are directed into the vacuum chamber. Each trapping laser beam has a power of ≈ 20 mW. A second amplified external-cavity laser system is used as a repumper. The trapped atoms are observed using a video camera, and we also image fluorescence from the atoms onto a linear diode array, enabling us to measure

the diameter of the cloud of atoms. We can measure the number of trapped atoms by measuring the fluorescence emitted into a known solid angle using a sensitive optical power meter. Using this apparatus we can trap up to 1.2×10^8 ^{85}Rb atoms in a spherical volume of diameter ≈ 1.2 mm (FWHM inferred from diode array signal). The maximum cold-atom number density is therefore $\sim 5 \times 10^{10} \text{ cm}^{-3}$. Rubidium atoms trapped by this method typically have temperatures of $\sim 100 \mu\text{K}$, corresponding to collision velocities of atom pairs of ~ 0.2 m/s.

Data Acquisition

The atoms are trapped midway between two parallel field plates made from high-transparency stainless steel mesh. Excitation of $5p_{3/2}$ atoms to a Rydberg state is achieved using a tunable pulsed laser (10 ns pulse length), and this state can then be field ionized at a specified delay after excitation using a ~ 1000 V, 1 μs rise time voltage pulse applied to the parallel meshes. (If a plasma forms, then ions or electrons from the plasma are also swept towards the MCP by the field ionization pulse.) The resulting ions or electrons are detected using the MCP. When electrons are detected, their time-of-flight to the detector is negligible, and the actual arrival time is determined by the time at which the voltage pulse reaches the electric field needed to ionize a particular Rydberg state. In general, therefore, electrons arriving at the MCP at later times come from states that are more deeply bound, though the time spectrum is also sensitive to the angular momentum of the state [23]. The electron time-of-flight spectrum can therefore reveal information on Rydberg population distribution, and also can be used to gain information about the energy spectrum of the plasma electrons.

Lasers

Excitation of optical transitions of cold atoms presents certain technological issues that must be considered. The Doppler width of an optical transition for a $100 \mu\text{K}$ Rb atom is less than 1 MHz, and therefore the spectral width of most transitions is limited by the upper and lower state lifetimes. For transitions from the $5p_{3/2}$ (the upper level of the trapping transition) to a Rydberg state, the limit is the $5p_{3/2}$ state's 5 MHz natural width. When exciting cold Rydberg atoms using ~ 10 ns pulsed dye lasers shot-to-shot fluctuations in the Rydberg population are generally close to 100% due mainly to the poor spectral overlap between the longitudinal modes of the dye laser and the transition spectral width. Generally, in each laser shot, several laser modes will oscillate within a bandwidth of $\sim 0.1 \text{ cm}^{-1}$, and the width of each mode will be ~ 100 MHz. From one shot to the next, the intensities of each mode will change, but more significantly, the frequency of each mode will change. Hence, not only is the spectral overlap of a laser mode with the transition poor, but it changes on a shot-to-shot basis.

To obtain relatively stable Rydberg state populations using a pulsed laser system, we have built a frequency doubled, pulse-amplified cw laser system based on an external cavity diode laser (this laser is termed the "narrow line width laser" in the rest of

this paper). Our system is based on a home-made external cavity diode laser operating around 960 nm. The output power from the laser cavity is 5 mW, and the spectral width is ≤ 10 MHz. Operation of the external cavity laser is monitored with a scanning confocal etalon, and the wavelength is measured using a commercial wavemeter. After passing through a 40 dB optical isolator, the light from the diode laser is amplified in three dye cells (LDS 925) pumped with the 532 nm light from a Nd:YAG laser, and then frequency doubled to 480 nm in a KNiO₃ crystal. The doubled output is 20 - 40 μ J per pulse, with a spectral width that is Fourier transform limited by the 10 ns YAG pulse to approximately 100 MHz. (We can easily discriminate between the Rb $32d_{3/2}$ and $32d_{5/2}$ states which are separated by 370 MHz.) Using this system, the shot-to-shot variation in the Rydberg signal is $< \pm 10\%$. The laser can be coarsely tuned to the vicinity of a transition using the wavemeter, and fine tuning is done by changing the voltage to a piezoelectric crystal that moves the diffraction grating in the external cavity diode laser.

We use a second pulsed laser to photoionize the cold atoms directly. This laser, which excites atoms in the $5p_{3/2}$ state to the continuum, is a Littman-type dye laser, pumped using the third harmonic 355 nm light from the Nd:YAG laser. Since it excites to the continuum, the frequency fluctuations cause no shot-to-shot variation in the number of ions formed, although there may be some small variation in the ion density due to the energy per pulse. In our experiments we investigate the effect of embedding Rydberg atoms in a pre-existing plasma on the plasma electron energy spectrum. Hence, the Littman laser first creates a plasma, and then, approximately 15 ns later, the frequency doubled, pulse-amplified cw laser system is used to excite to a specific Rydberg state.

Using the narrow bandwidth laser system, we estimate we can create a maximum Rydberg density of $1 \times 10^{10} \text{ cm}^{-3}$. However, our estimates of absolute Rydberg atom population densities have an uncertainty of a factor of 3, though relative populations can be measured to 10%.

RESULTS

In the following two sections, we describe our preliminary results. First, we describe experiments where only the narrow line width laser was used to create a Rydberg sample which then evolved to a plasma. Second, we describe our results on the effect of adding Rydberg atoms into a pre-existing plasma. In this second set of results, we see possible evidence that the Rydberg atoms do, in fact, stabilize the plasma.

Evolution of Rydberg Atoms to Plasma

Our preliminary experiments investigated the evolution of Rydberg states to plasma. These experiments used only our narrow line width frequency doubled, dye amplified diode laser system to excite a selected Rydberg state, and were carried out as a test of the narrow line width laser system's ability to make dense Rydberg samples. They also offer information on the behavior of a plasma that evolves from a Rydberg sample. Results of these experiments are shown in Figs. 1 and 2.

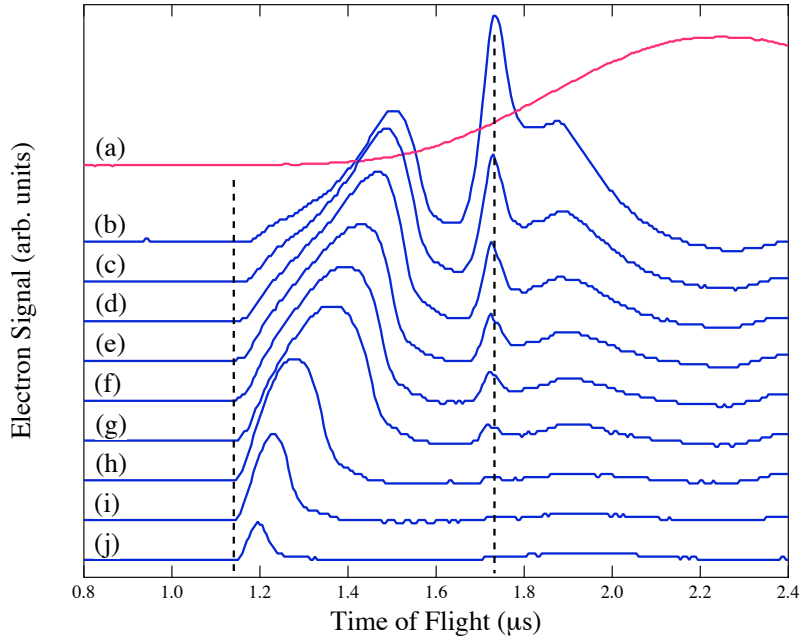


FIGURE 1. Electron time-of-flight signal from field ionization (FI) of a dense sample of ultra cold rubidium atoms in the $40d_{5/2}$ state, and the plasma to which this state evolves. The atom density is $\approx 1 \times 10^{10} \text{ cm}^{-3}$, and the signals are shown as a function of delay between the laser pulse that excites the $40d_{5/2}$ state and the beginning of the FI pulse (the FI pulse rise-time is $\approx 1 \mu\text{s}$). From top to bottom: (a) the FI pulse (different vertical units), and then the signals from the various delays: $0 \mu\text{s}$ (b), $2 \mu\text{s}$ (c), $4 \mu\text{s}$ (d), $6 \mu\text{s}$ (e), $8 \mu\text{s}$ (f), $10 \mu\text{s}$ (g), $20 \mu\text{s}$ (h), $30 \mu\text{s}$ (i), and $40 \mu\text{s}$ (j). The vertical axis scale is the same for all graphs, except for the FI pulse. The vertical dashed line at approximately $1.7 \mu\text{s}$ marks the adiabatic threshold for $40d_{5/2}$, and the dashed line at $1.15 \mu\text{s}$ locates the beginning of the FI pulse. The large “hump” between $1.15 \mu\text{s}$ and $1.6 \mu\text{s}$ in (b), and which moves progressively towards $1.15 \mu\text{s}$ as the delay increases, is due to electrons from the plasma and high- n Rydberg states.

We first investigated the evolution of the $40d_{5/2}$ Rydberg state population, and the resulting plasma, as a function of delay between the laser pulse and the application of the field ionization pulse from zero to $40 \mu\text{s}$. These results are shown in Fig. 1, and are basically similar to previously published work (see, for example Ref. [24]). As can be seen, there is already a robust plasma that forms within $1 \mu\text{s}$ of the $40d_{5/2}$ state excitation, and the plasma is quite deeply bound (this is the large “hump” between $1.15 \mu\text{s}$ and $1.6 \mu\text{s}$ in Fig. 1(b)). In fact, it takes an electric field of 78 V/cm (sufficient to adiabatically field ionize a state of quantum number $n^* = 45$) to remove the last electrons from the plasma. It should be pointed out, however, that the field ionization technique cannot distinguish a plasma signal from that due to field ionization of Rydberg states. Secondly, it is difficult to extract quantitative information from the plasma signal obtained using our method without thorough modeling of the plasma dynamics. The reason for this is that, as the voltage pulse removes the least strongly bound electrons from the plasma, those left become even more strongly bound to the positive ions. We will ultimately circumvent this problem by using the electron spilling technique to measure the electron temperature [18].

As the delay increases, the Rydberg signal from $40d_{5/2}$ decreases significantly, and the plasma expands slowly due to the Coulomb repulsion of the ions. As it expands, the potential well depth decreases, and the more energetic electrons escape. The plasma signal gets smaller and migrates to lower flight times, characteristic of needing a smaller electric field to quench the plasma. One other feature visible in the time-of-flight spectra is the pronounced “hump” after the $40d_{5/2}$ adiabatic ionization signal (flight time $> 1.8 \mu\text{s}$). This is due to non-adiabatic ionization of $40d_{5/2}$, and both adiabatic and non-adiabatic ionization of angular momentum $\ell > 2$ states that are populated by elastic electron-Rydberg scattering, and also from states with $n < 40$ populated by inelastic electron-Rydberg encounters [6]. Population of such states is necessary to maintain the energy balance in the system, enabling some of the Rydberg atoms to ionize and form the plasma. One interesting point that has been noted previously is that there appears to be some stabilization of the plasma due to the Rydberg atoms [24]. It is only when the $40d_{5/2}$ population effectively vanishes (at a delay of $20 \mu\text{s}$, Fig. 1(h)), that the plasma really starts to dissipate.

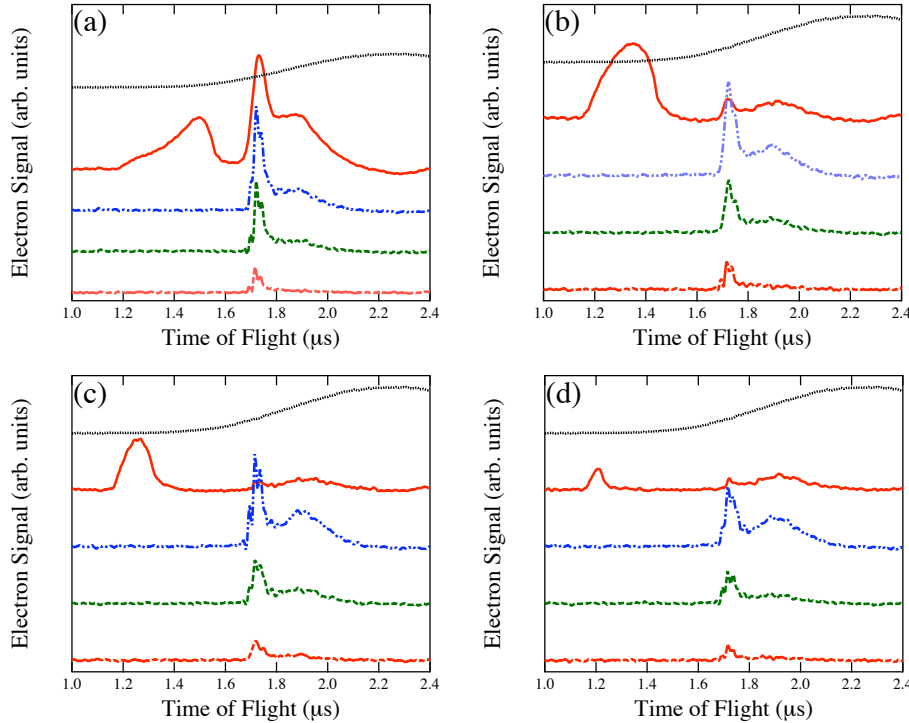


FIGURE 2. Electron time-of-flight signals from field ionization (FI) of a dense sample of ultra cold rubidium atoms in the $40d_{5/2}$ state, and the plasma to which this state evolves. The signals are shown for different delays between the laser and the FI pulse, and at different densities. The respective delays are $0 \mu\text{s}$ (a), $10 \mu\text{s}$ (b), $20 \mu\text{s}$ (c), and $30 \mu\text{s}$ (d). Within each graph, from top to bottom, the following data are displayed: the FI pulse (black \cdots , different vertical units); FI signal at an initial Rydberg density of $1 \times 10^{10} \text{ cm}^{-3}$ (red solid line); $2 \times 10^9 \text{ cm}^{-3}$ (blue dash-dot); $1 \times 10^9 \text{ cm}^{-3}$ (green dashed), and $3 \times 10^8 \text{ cm}^{-3}$ (red long-dashed). The vertical axis scale is the same for all graphs, except for the FI pulse. The FI pulse turns on at $1.15 \mu\text{s}$, and the $40d_{5/2}$ state adiabatically ionizes at approximately $1.7 \mu\text{s}$.

We also investigated the density dependence of the evolution process. For four different delays between the laser and the field ionization pulse, we changed the Rydberg atom density by placing neutral density (ND) filters in the pulsed laser beam. The resulting Rydberg atom densities were $1 \times 10^{10} \text{ cm}^{-3}$ (no filter), $2 \times 10^9 \text{ cm}^{-3}$, $1 \times 10^9 \text{ cm}^{-3}$, and $3 \times 10^8 \text{ cm}^{-3}$. These results are shown in Fig. 2, again shown for the $40d_{5/2}$ state.

As can be seen, the Rydberg sample evolves to plasma only at the very highest density. However, even at lower density, there is evidence for population redistribution into $\ell > 2$, $n < 40$ states that ionize at higher fields than the adiabatic threshold for $40d_{5/2}$. It is likely that ionization is occurring at a low rate due to dipole forces at the lower densities, but that the excess positive charge density of the ions is never sufficient to form a plasma.

Two-Laser Experiments

The observation noted above, namely that the ultra cold plasma seems to be more stable when there is still a significant Rydberg density, motivated our two-laser experiments. In these, we used a pulsed Littman dye laser to photoionize a sample of cold Rb $5p_{3/2}$ atoms to create a plasma directly. At a delay of 15 ns, we used our narrow line width laser to populate the $40d_{5/2}$ state from cold atoms remaining in the $5p_{3/2}$ state. We then observed the evolution process of the sample as a function of delay from the pulsed laser. These data are shown in Fig. 3. In these experiments, we reduced the FI pulse amplitude so that it was large enough to quench the plasma, but not large enough to field ionize the $40d_{5/2}$ state. We did this to maintain as high a trap density as possible over the course of the experiment. The experiment is performed at 20 Hz, and a significant fraction of the cold atoms are either ionized, or excited to a Rydberg state. If we field ionize the Rydberg atoms, these cold atoms are removed from the trap, which doesn't refill fully before the next laser shot. Typically, in the experiments described above, our cold atom density decreases by 30% when we field ionize the Rydberg atoms. The Rydberg atom and plasma densities we can create are therefore significantly higher when we reduce our FI pulse so that only the plasma is quenched.

As can be seen, the plasma created by the Littman laser alone, in the absence of the narrow line width laser to populate the $40d_{5/2}$ state, not very robust (second trace from the bottom in each graph). The number of positive ions seems to be much lower than in the plasmas that evolve from a Rydberg state shown in Fig. 1, and as a result the plasma dissipates after only 15 μs . The reasons for this are unclear to us. Certainly, our Littman laser may not be as tightly focused as we think, but it may also be as a direct consequence of the n^{-3} decrease in the optical excitation cross section as the laser is tuned over the ionization limit. On the other hand, the plasma that forms by evolution from the $40d_{5/2}$ state only begins to appear after 5 μs , and reaches its maximum at 15 μs . When we illuminate the cold atoms with both the Littman laser, to create a plasma directly, and 15 ns later with the narrow line width laser to embed cold Rydberg atoms within the plasma, several things are apparent. First (and perhaps obviously), our technique in its present form is unable to distinguish whether, at short delays ($\leq 15 \mu\text{s}$), the pre-existing plasma accelerates the evolution of the subsequently created Rydberg atoms to plasma, or whether the Rydberg atoms stabilize the plasma in the first few hundred ns. What

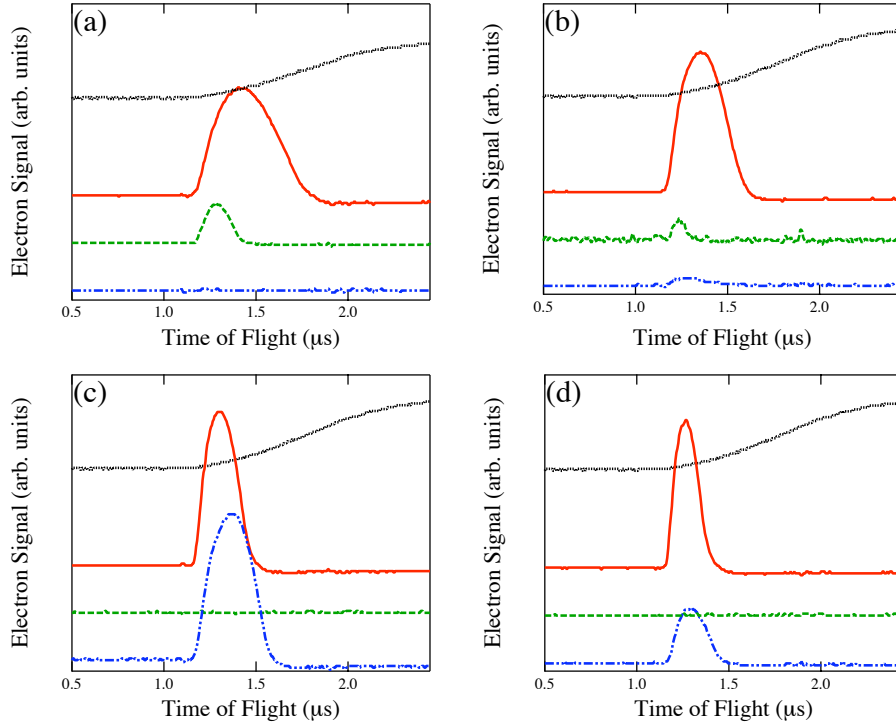


FIGURE 3. Electron time-of-flight signals from an ultra cold plasma formed by photoionization. The signals are shown for different delays between the laser and the FI pulse, and with- and without the presence of cold Rydberg atoms. The respective delays are $5 \mu\text{s}$ (a), $15 \mu\text{s}$ (a), $25 \mu\text{s}$ (a), and $35 \mu\text{s}$ (d). Within each graph, from top to bottom, the following data are displayed: the FI pulse (black \cdots , different vertical units); plasma signal when Littman laser creates the plasma and the narrow line width laser excites the $40d_{5/2}$ state 15 ns later (red solid line); signal from plasma formed by Littman laser alone, with no narrow band width laser to create Rydberg atoms (green $---$), and the plasma signal from the evolution of the $40d_{5/2}$ state created by the narrow line width laser, and no Littman laser to create the plasma directly (blue $- \cdot -$). The vertical axis scale is the same for all graphs, except for the FI pulse. The FI pulse turns on at $1.15 \mu\text{s}$, and the FI pulse amplitude was not large enough to adiabatically ionize the $40d_{5/2}$ state.

is clear is that the plasma that forms when both lasers are used is much more robust than that due to the Littman laser alone, and its formation is accelerated by some $10 \mu\text{s}$ from the corresponding stage of a plasma that evolves from a Rydberg sample, with no pre-existing plasma from the Littman laser.

We believe the data shown in Fig. 3 reveal preliminary evidence that the presence of cold Rydberg atoms embedded within the plasma are cooling and stabilizing the plasma, and therefore slowing the plasma expansion and leading to a longer plasma lifetime. This can be seen in Figs. 3(c) and (d) by the fact that the plasma created by the Littman laser, and moderated by the presence of Rydberg atoms from the narrow line width laser, changes only a small amount in the $10 \mu\text{s}$ from (c) to (d), whereas the plasma that evolves from a cold Rydberg sample alone has expanded and the positive ion well depth has declined by approximately 60%. Briefly, the two-laser plasma is accelerated (takes a smaller amount of time after creation to reach a certain charge density) from that evolving from a cold Rydberg sample, and is sustained longer.

CONCLUSION

We believe we see tentative evidence to support the suggestion that Rydberg atoms may be used to cool the electron temperature in an ultra cold plasma. Further work is required to observe the effect of changing the Rydberg density, using other Rydberg states, and changing the delay between the plasma creation laser and the Rydberg laser. Further, better characterization of the electron temperature will be necessary.

ACKNOWLEDGMENTS

Funding for this work has come from the National Science Foundation and Colby College through the Division of Natural Sciences Grant Program. We acknowledge discussions with Charlie Conover, Paul Tanner, and Tom Gallagher. Valuable assistance has been provided by Andrew Kortyna, Mao Zheng, and Drew Branden.

REFERENCES

1. T. C. Killian, S. Kulin, S. D. Bergeson, L. A. Orozco, C. Orzel, and S. L. Rolston, *Phys. Rev. Lett.* **83**, 4776 (1999).
2. D. Feldbaum, N. Morrow, S. K. Dutta, and G. Raithel, *Phys. Rev. Lett.* **89**, 173004 (2002).
3. N. Vanhaecke, D. Comparat, D. A. Tate, and P. Pillet, *Phys. Rev. A* **71**, 013416 (2005).
4. C. E. Simien, Y. C. Chen, S. Laha, P. Gupta, Y. N. Martinez, P. G. Mikelson, S. B. Nagel, and T. C. Killian, *Phys. Rev. Lett.* **92**, 143001 (2004).
5. F. Robicheaux, and J. D. Hanson, *Phys. Rev. Lett.* **88**, 055002 (2002).
6. F. Robicheaux, and J. D. Hanson, *Phys. Plasmas* **10**, 2217 (2003).
7. S. Mazevet, L. A. Collins, and J. D. Kress, *Phys. Rev. Lett.* **88**, 055001 (2002).
8. S. Bergeson, and R. L. Spencer, *Phys. Rev. E* **67**, 026414 (2003).
9. T. Pohl, and T. Pattard (2005), [arXiv:physics/0503018](https://arxiv.org/abs/physics/0503018).
10. T. Pohl, T. Pattard, and J. M. Rost, *Phys. Rev. Lett.* **94**, 205003 (2005).
11. M. P. Robinson, B. L. Tolra, M. W. Noel, T. F. Gallagher, and P. Pillet, *Phys. Rev. Lett.* **85**, 4466 (2000).
12. T. F. Gallagher, P. Pillet, M. P. Robinson, B. Laburthe-Tolra, and M. W. Noel, *J. Opt. Soc. Am. B* **20**, 1091 (2003).
13. W. Li, M. W. Noel, M. P. Robinson, P. J. Tanner, T. F. Gallagher, D. Comparat, B. Laburthe-Tolra, T. Vogt, N. Zahzam, N. Vanhaecke, P. Pillet and D. A. Tate, *Phys. Rev. A* **70**, 042713 (2004).
14. W. Li, P. J. Tanner, and T. F. Gallagher, *Phys. Rev. Lett.* **94**, 173001 (2005).
15. W. Li, P. J. Tanner, Y. Jamil, and T. F. Gallagher, *Eur. Phys. J. D* **40**, 27 (2006).
16. S. Ichimaru, *Rev. Mod. Phys.* **54**, 1017 (1982).
17. T. Pohl, D. Comparat, N. Zahzam, T. Vogt, P. Pillet, and T. Pattard, *Eur. Phys. J. D* **40**, 45 (2006).
18. J. L. Roberts, C. D. Fertig, M. J. Lim, and S. L. Rolston, *Phys. Rev. Lett.* **92**, 253003 (2004).
19. C. Monroe, W. Swann, H. Robinson, and C. Wieman, *Phys. Rev. Lett.* **65**, 1571 (1990).
20. W. R. Anderson, J. R. Veale, and T. F. Gallagher, *Phys. Rev. Lett.* **80**, 249 (1998).
21. I. Mourachko, D. Comparat, F. de Tomasi, A. Fioretti, P. Nosbaum, V. M. Akulin, and P. Pillet, *Phys. Rev. Lett.* **80**, 253 (1998).
22. A. S. Arnold, J. S. Wilson, and M. G. Boshier, *Opt. Commun.* **69**, 1236 (1998).
23. T. H. Jeys, G. W. Foltz, K. A. Smith, E. J. Beiting, F. G. Kellert, F. B. Dunning, and R. F. Stebbings, *Phys. Rev. Lett.* **44**, 390 (1980).
24. W. Li, M. W. Noel, M. P. Robinson, P. J. Tanner, T. F. Gallagher, D. Comparat, B. Laburthe-Tolra, T. Vogt, N. Zahzam, N. Vanhaecke, P. Pillet, and D. A. Tate, *Phys. Rev. A* **70**, 042713 (2004).